Proceedings World Geothermal Congress 2020+1
Reykjavik, Iceland, April - October 2021

Energy and Exergetic Analysis of a Proposed Olkaria I Binary Geothermal Power Plant, Naivasha, Kenya

Alvin K. Bett, Eric K Rop, Saeid Jalilinasrabady and Ryuchi Itoi

iklaeb@gmail.com

abett@jkuat.ac.ke

Keywords: *binary, geothermal, energy, exergy, efficiency*

ABSTRACT

Olkaria I geothermal power plant in Kenya has an installation capacity of 45 MWe. This single-flash power plant has exergy waste of about 6 MWe in the separated brine. To maximize the geothermal resource, a binary unit using isobutene as a working fluid was developed and optimized using Engineers Equation Solver code. The paper presents the design and energy and exergy analysis of the proposed binary unit for the Olkaria I power plant. The designed binary plant has the potential of generating net turbine work of 2281 kW with plant efficiency of 10.81%, cycle efficiency of 9.87%, and overall utilization efficiency of 31.70%. The temperature of brine reinjected into the reservoir was set at 85 °C with exergy of 1763 kW. A Grassman exergy flow diagram shows that exergy destruction is greatest in the condenser (12.08%) and least in the evaporator (8.99%). Energy and exergy analysis of a plant help to optimize available geothermal resources for maximum energy production.

1. INTRODUCTION

Geothermal energy is available around the world. A geothermal resource needs a large heat source, permeable reservoir, water supply, cap rock, and reliable recharge mechanism to be commercially viable (DiPippo, 2014). The growth of the world population has increased the world energy demand and thus the need to maximize the use of available resources (Jalilinasrabady, et al., 2012). The increasing demand calls for the sustainable development of energy sources and the detailed analysis of systems (Kwambai, 2010; Jalilinasrabady, 2011).

The single-flash Olkaria I geothermal power plant is located in the Olkaria geothermal area in Naivasha, Kenya, as shown in Figure 1. The plant has three condensing steam turbine units, each with a rating of 15 MWe and generating 45 MWe in total, and is owned by the Kenya Electricity Generating Company (KENGEN). Figure 2: Flow diagram of the Olkaria I power plant presents a diagram of the overall flow of the plant. The detailed energy and exergy analysis of the entire power plant is presented in Table 1.

Table 2 shows that geothermal brine has potential exergy of 6 MWe and a flow rate of the brine of 67.14 kg/s at pressure of 6 bars. The objective of the study was to investigate the technical feasibility of constructing a 2-MW commercial geothermal power plant.

Table 1: Summary of the exergy analysis of the Olkaria I power plan (Kwambai, 2005).

PROCESS/SYSTEM	TOTAL EXERGY (MW)	DESIRED EXERGY OUTPUT (MW)	WASTED EXERGY OUTPUT (MW)	EXERGY DESTROYED (MW)	EXERGY EFFICIENCY (%)
SEPARATION	109	103	6		96
TRANSMISSION	103	92	11		90
TURBINES	89	49	30	10	84
CONDENSER	30	15	1	14	52
GES	1.89	0.33	1.56	-	17
COOLING SYSTEM	0.5	7		7 (desired)	11.3
OVERALL	135	44.7		90	34

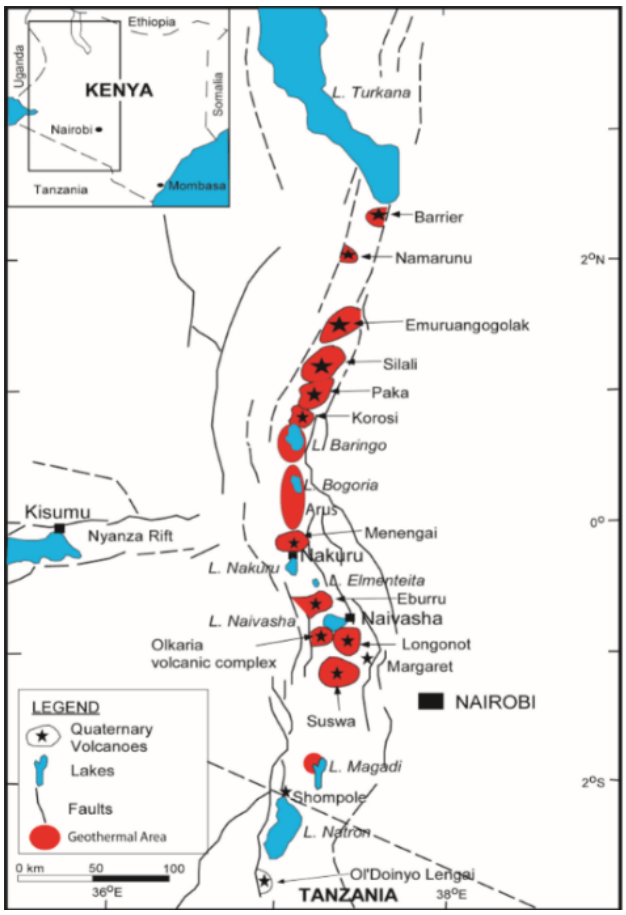

Figure 1: Map of Kenya showing the location of the Olkaria geothermal area (Kwambai, 2010).

Table 2: Output parameters of the Olkaria I power plant (Kwambai, 2005).

Well No OW-	Discharge WHP (bar-a)	Separator pressure (bar-a)	Enthalpy (kJ/kg)	Steam flow (kg/s)	Water flow (kg/s)	Quality	Status 30/7/05
2	7.00	6.20	2168	4.64	1.81	0.72	**On**
5	7.05	6.40	2313	12.39	3.39	0.79	**On**
8	6.00	5.90	2486	6.44	0.94	0.87	**Shut**
10	6.35	5.80	2520	4.06	0.50	0.89	**Shut**
11	7.00	6.00	1941	3.94	1.92	0.67	**On**
13	6.10	5.90	2614	3.47	0.25	0.93	**Shut**
15	6.10	5.60	2034	5.64	2.94	0.66	**On**
16	6.00	5.80	1444	8.08	13.61	0.37	**On**
18	6.00	6.00	2663	6.50	0.31	0.96	**On**
19	8.50	5.80	1912	5.36	3.58	0.60	**On**
20	6.00	6.00	2595	5.64	0.47	0.92	**Shut**
21	6.20	5.80	2228	3.83	1.28	0.75	**Shut**
22	6.00	6.10	1746	3.64	3.39	0.52	**Shut**
23	6.30	6.20	2104	4.22	1.89	0.69	**Shut**
24/28	6.50,9.0	6.30	2539	9.81	1.14	0.90	**On**
25	9.50	6.20	2219	3.81	1.33	0.74	**Shut**
26	8.50	8.20	1856	9.69	7.75	0.56	**On**
27/31/33	6.5,7.5,7.0	5.10	2481	18.97	2.83	0.87	**Shut**
29/30	10.3,9.50	5.10	2398	39.94	8.44	0.83	**On**
32	7.20	6.80	2335	36.28	9.36	0.79	**On**
Mean/Total	**7.17**	**6.06**	**2229.8**	**196.36**	**67.14**	**0.75**	

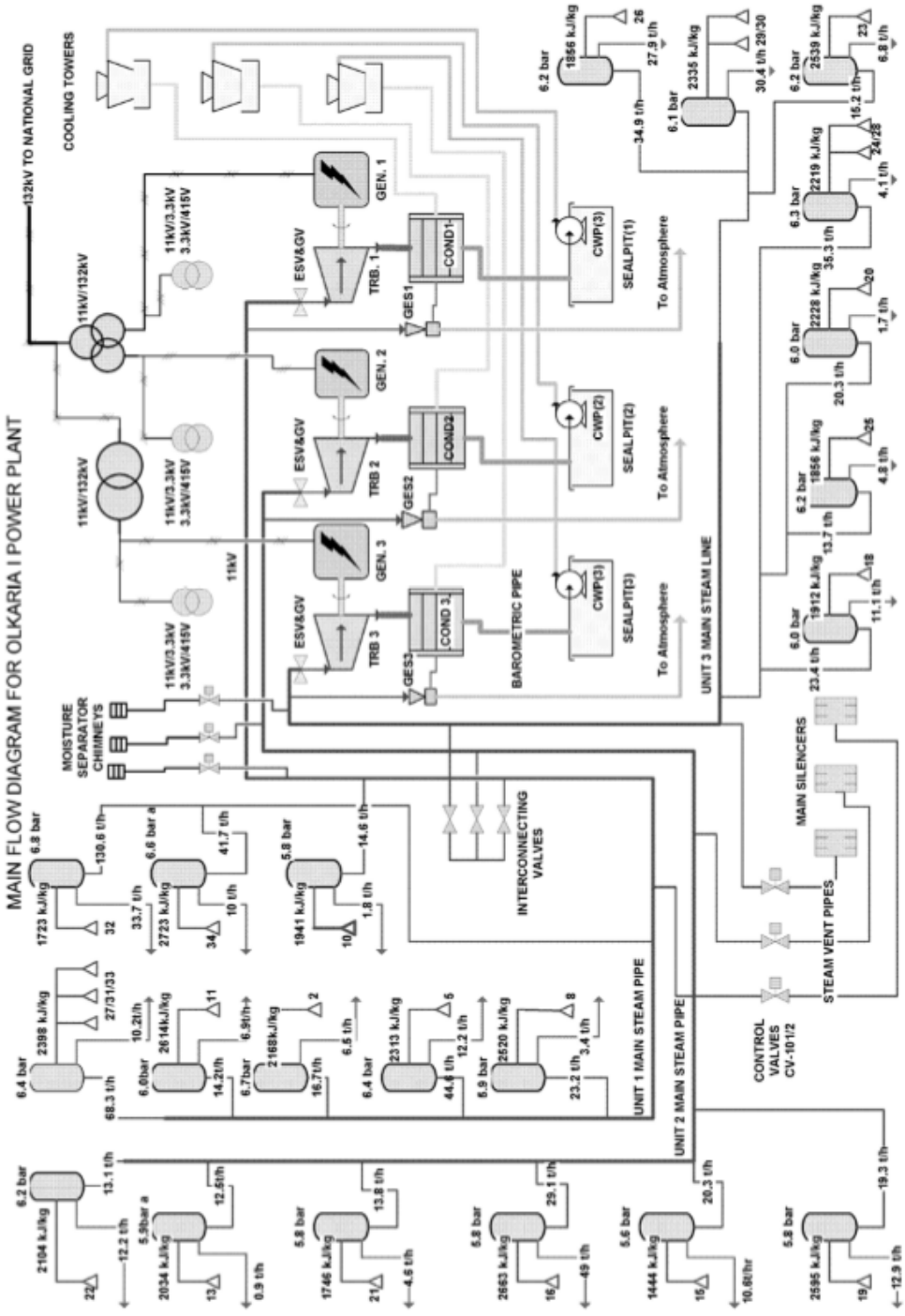

Figure 2: Flow diagram of the Olkaria I power plant (Kwambai, 2005).

Specific objectives were to conduct an exergy analysis of the Olkaria I power plant, to propose and design a binary plant for the Olkaria I power plant, and to carry out energy and exergy analysis of the binary plant using Engineers Equation Solver (EES) code.

2. BINARY POWER PLANT

A binary geothermal power plant has a working fluid that undergoes a closed cycle. The selected working fluid receives heat from the geothermal fluid, evaporates, expands through a turbine, condenses, and completes its cycle in the evaporator via the use of a feed pump (DiPippo, 2014). Most flash-steam plants are currently adding binary units to maximize the available energy and thus improve the utilization efficiency of geothermal resources. Low-temperature geofluids are also used for binary units and direct uses. Binary units can use heat more effectively than a single flash in terms of the enthalpy of the waste geothermal fluid (Sadiq & Moon, 2014).

Candidates for the working fluid vary according to thermodynamic properties, health, safety, and environmental impacts. Table 3 shows relevant thermodynamic and health and environmental properties of working fluids. The properties of the fluids can be compared with those of pure water (DiPippo, 2012; Jalilinasrabady, 2011).

Table 3: Thermodynamic and environmental properties of potential working fluids.

Fluid	Formula	T_c (^{0}C)	P_c (MPa)	Toxicity	Flammability	ODP	GWP
Propane	C_3H_8	96.95	4.236	low	Very high	0	3
i-Butane	i-C_4H_{10}	135.92	3.685	low	Very high	0	3
n-Butane	C_4H_{10}	150.8	3.718	low	Very high	0	3
i-Pentane	i-C_5H_{12}	187.8	3.409	low	Very high	0	3
n-Pentane	C_5H_{12}	193.9	3.240	low	Very high	0	3
Ammonia	NH_3	133.65	11.627	toxic	Lower	0	0
Water	H_2O	374.14	22.089	Non-toxic	Non-flammable	0	-

The ozone depletion potential (ODP) is normalized at 1.0 for banned refrigerant R-11 and the global warming potential (GWP) is normalized at 1.0 for carbon dioxide (DiPippo, 2014).

3. LAWS OF THERMODYNAMICS

The first law of thermodynamics quantifies energy (Kumar, et al., 2016) and states that energy is conserved during any process as it is transformed from one form to another (Jalilinasrabady, et al., 2010; DiPippo, 2012). Any system that is not in equilibrium with its surroundings owing to differences in temperature, pressure, or chemical composition has the potential to do work (Kwambai, 2005).

The first law of thermodynamics for a system is given as:

$$\dot{Q} - \dot{W} = \dot{m}[(h_2 - h_1) + 1/2(v_2^2 - v_1^2) + g(z_2 - z_1)] \quad (1)$$

By ignoring the kinetic and potential energy differences related to the enthalpy difference, Eq. (1) is expressed as:

$$\dot{Q} - \dot{W} = \dot{m}(h_2 - h_1) \quad (2)$$

The second law of thermodynamics for a given system and its surroundings is given by

$$\dot{\theta} = \dot{m}(s_2 - s_1) - \dot{Q}/T_0 \quad (3)$$

Entropy production is zero for an ideal reversible operation. From Eqs. (2) and (3), the maximum work is obtained as

$$\dot{W}_{max} = \dot{m}[(h_1 - h_2) - T_0(s_1 - s_2)] \quad (4)$$

4. METHODOLOGY

4.1 System Description of the Proposed Binary Power Plant for Olkaria I

Figure 3 illustrates schematic flow diagram of the proposed Olkaria I binary unit. The brine separated by the separator enters the evaporator in Step 1 indicated in the diagram as 1 and goes through the evaporator in Step 2 to flow to reinjection wells. Working fluid (Step 8) passes through the evaporator and is converted to vapor (Step 3). The saturated vapor of working fluid expands in the turbine from high pressure P_3 to low pressure P_4 to generate electricity (Steps 3 and 4). Steps 4 and 5 are preheating the working fluid to its boiling point for use in Steps 7 and 8. The exhaust vapor is condensed to liquid in the condenser in Steps 5 and 6, and then pumped to high pressure P_3 through the regenerator and evaporator by the feed pump, State 6. For the thermodynamic analysis; Figure 4 shows the T–s diagram of the cycle.

The assumptions made are:

- saturated liquid of the working fluid at the condenser outlet;
- isentropic pump and turbine efficiencies of 75% and 85% respectively.

4.2 Turbine

Figure 4 shows that the vapor undergoes isentropic expansion in the turbine (Steps 3 and 4). P-h diagram of isobutene, Figure 8 illustrates the critical pressure of the working fluid and the corresponding enthalpy.

$$s_4 = s_3 \quad (5)$$

With fixed pressure P4 and entropy s4 after the turbine, the enthalpy of the working fluid is calculated using EES code. With the enthalpies of Steps 3 and 4, the turbine power output, $\dot{W}t$, is obtained as:

$$\dot{W}_t = (h_3 - h_4)\dot{m}_{wf}\eta_t \quad (1)$$

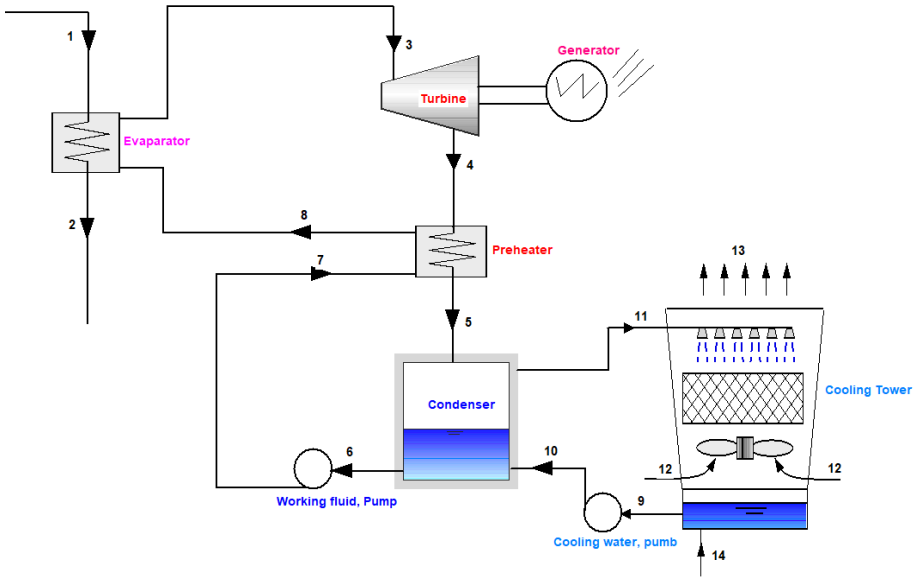

Figure 3: Schematic diagram of an ORC plant (modeled using EES code).

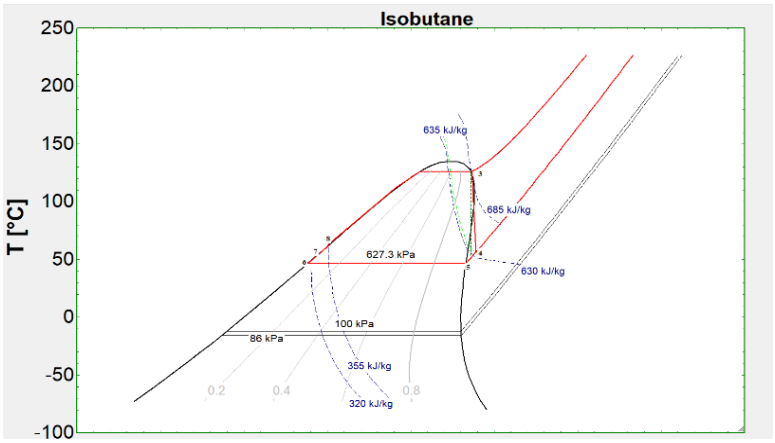

Figure 4: T–s diagram illustrating the flow process of working fluid

4.3 Heat Exchangers

Thermal energy in the heat exchangers is transferred from one fluid to another. Three heat exchangers (evaporator, preheater condenser) are analyzed. It is assumed that all heat exchangers are well insulated so that all heat is transferred between the fluids (DiPippo, 2012). Geothermal brine transfers some of the energy, Q_{in}, to the working fluid in the evaporator. Considering a steady flow, the governing equations are:

$$Q_{in} = \dot{m}_b C_b (T_1 - T_2) \tag{2}$$

$$(h_3 - h_8)\dot{m}_{wf} = \dot{m}_b C_b (T_1 - T_2) \tag{3}$$

$$\dot{m}_{wf} = \frac{Q_{in}}{(h_3 - h_8)} \tag{4}$$

where C_b (kJ/kg K) is the specific heat capacity of the geothermal fluid, T_1 and T_2 are respectively inlet and outlet temperatures of separated brine in the evaporator, and $\dot{m}_b$ is the mass flow rate of the brine.

The preheater transfers heat from exhaust vapor of the turbine to cold liquid of the feed pump. For the preheater, the heat transfer Q_{PH} is given by:

$$Q_{PH} = \dot{m}_{wf}(h_4 - h_5). \tag{5}$$

A water-cooled condenser is used to condense the low-temperature exhaust vapor from the preheater. The condenser temperature was set to 46.5 °C (DiPippo, 2012; Jalilinasrabady, et al., 2011; Yajing & Jianfeng, 2016). The heat rejected from the working fluid to the cooling water from the cooling tower is:

$$Q_c = \dot{m}_{wf}(h_5 - h_6) \tag{6}$$

The relationships of the flow rates of the working fluid $\dot{m}_{wf}$ and cooling water $\dot{m}_{cw}$ are:

$$(h_5 - h_6)\dot{m}_{wf} = \dot{m}_{cw}(h_{11} - h_{10}) \tag{7}$$

$$(h_5 - h_6)\dot{m}_{wf} = \dot{m}_{cw}C_{cw}(T_{11} - T_{10}) \tag{8}$$

where C_{cw} is the specific heat capacity of the cooling water. From Eq. (13), the mass flow rate of the cooling water for the dissipation of the waste heat can be determined for a cooling tower with a temperature range of $T_{11} - T_{10}$, (DiPippo, 2012).

4.4 Pump of the system

Power imparted to the working fluid (Steps 6 and 7) by the feed pump is:

$$\dot{W}_{pwf} = \frac{(h_7 - h_6)\dot{m}_{wf}}{\eta_p} \tag{9}$$

while cooling water pump power (Steps 9 and 10) is:

$$\dot{W}_{pcw} = \frac{(h_{10} - h_9)\dot{m}_{cw}}{\eta_p} \tag{10}$$

where η_p is the efficiency of the isentropic pump (DiPippo, 2012). The pump power is referred to as parasitic loads and reduces the turbine work to obtain the net work (Eq. 16) of the plant.

$$\dot{W}_{net} = \dot{W}_t - \left(\dot{W}_{pwf} + \dot{W}_{pcw}\right) \tag{11}$$

4.5 Plant efficiency

According to the first law of thermodynamics, the cycle performance is assessed in terms of thermal efficiency as:

$$\eta_{th} = W_{net}/Q_{in} \tag{12}$$

The thermal efficiency is the difference between the thermal input power and thermal rejected power of the system, and Eq. (17) is thus rewritten as (DiPippo, 2012):

$$\eta_{th} = 1 - \frac{Q_c}{Q_{in}} \tag{13}$$

For commercial purposes, the plant efficiency and utilization efficiency need to be calculated and presented to investors and other interested business partners for decisions to be made according to the return of investment.

4.6 Selection of working fluid and system optimization

In conversion of geothermal heat source for electricity generation using ORC cycles the working fluid selection is a major design choice to maximize the plant performance (Manente & Lazzaretto, 2012). A number of working fluids can be selected from Table 3. The critical temperatures of propane, isobutene, n-butane, ammonia, and isopentane are 96.95, 135.92, 150.8, 133.65, and 187.8°C respectively. According to the data available, the geofluid temperature after separation is 157°C. Among the five potential organic fluids, isobutane, propane, and ammonia are the most suitable. Owing to its toxicity, ammonia is excluded on environmental considerations. Propane and isobutene have approximately the same heat transfer coefficients but different critical pressures, P_c (DiPippo, 2012). Isobutane was selected as the working fluid with consideration of the pressure and overall plant efficiency.

Plant optimization involves the input of various parameters, namely the turbine isentropic efficiency, working fluid flow rate, turbine and condenser operating pressures, and reinjection temperature of the brine.

The reference environment for the analysis is the Olkaria area with ambient temperature T_0 of 20°C and P_0 of 0.86 bar. Exergy analysis of the Olkaria I power plant by Kwambai gave condenser mean temperatures of 25°C and 38°C for the inlet cooling water and outlet water flowing to the cooling tower, respectively (Kwambai, 2005). The main constraints considered in the optimization of the plant are a brine flow rate of 67 kg/s, reinjection temperature of 85°C, and condenser temperature T_5 of 46.5°C. The objective function is maximum net work generated by the turbine. The maximum work was achieved by varying the high pressure P_3 to get the optimum pressure to run the isobutane ORC cycle.

5. ENERGY AND EXERGY ANALYSIS OF THE SYSTEM

Exergy is a powerful concept in the assessment of the performance of power plants (Anon., 2010). Exergy is considered by applying the second law of thermodynamic analysis to gauge the performance of, and compare geothermal power plants with other conventional plants (Kwambai, 2005; Jalilinasrabady, 2011).

Exergy is the maximum power output that can be theoretically obtained from a substance at specified thermodynamics conditions relative to its surroundings (DiPippo, 2012).

Various parameters were investigated to optimize the proposed model for maximum possible power output. Input variables included the working fluid flow rate and turbine inlet and outlet pressures (P_3 and P_4) (Jalilinasrabady, et al., 2011). The preheater temperature T_8 was optimized in EES software by fixing the working fluid flow rate and reinjection temperature, T_2. For the Olkaria geothermal field, no major cases of scaling have been reported and the waste brine temperature was set to 85°C.

By designing a system such that the final geofluid state is identical to the ambient surroundings, the exergy for a given initial state is:

$$\dot{E} = \dot{m}[h_1 - h_0 - T_0(s_1 - s_0)] \tag{14}$$

For system components, exergy input is the sum of exergy output and exergy destroyed. Each component of the plant was analyzed in terms of the available and destroyed exergy.

5.1 Evaporator

The exergy input to the heat exchanger is the summation of the brine exergy in State 1 and the working fluid in State 8. Meanwhile, the exergies leaving the heat exchanger are the exergies of States 2 and 3 for the geothermal fluid and working fluid respectively. Geofluid exergy in State 1 is the total available exergy for the binary plant and is fixed depending on the brine temperature as it exits the separator. The other exergies in the evaporator depend on the turbine high and low pressures (for States 3 and 8) and the reinjection temperature T_2. Exergy equation is:

$$\dot{E_1} = \dot{E_2} + \dot{E_3} - \dot{E_8} + \dot{E_{EvX}} \tag{15}$$

where $\dot{E_1}$ is the brine exergy (i.e., total available energy), $\dot{E_2}$ is the exergy of the brine water reinjected into the reservoir, $\dot{E_3}$ is the exergy of isobutane exiting the evaporator into the turbine, $\dot{E_8}$ is the exergy of isobutane entering the evaporator, and $\dot{E_{EvX}}$ is the exergy destroyed in the evaporator.

5.2 Turbine Analysis

The steam flow is converted into useful work in the turbine (Kumar, et al., 2016). During expansion, the available exergy in State 3 is converted to mechanical work by rotating the generator to generate electricity. The exergy balance in the turbine is given as:

$$\dot{E}_3 = \dot{E}_4 + \dot{E}_{WTurbine} + \dot{E}_{TX} \tag{16}$$

where $\dot{E}_3$ is the exergy of isobutene vapor entering the turbine, $\dot{E}_4$ is the exergy exiting the turbine, $\dot{E}_{WTurbine}$ is the turbine gross work, and $\dot{E}_{TX}$ is the exergy destruction rate in the turbine.

5.3 Preheater

The preheater transfers heat from the isobutane vapor to the isobutane fluid as the flow passes from State 4 to State 8:

$$\dot{E_4} = \dot{E_5} + \dot{E_8} - \dot{E_7} + \dot{E_{PHX}} \tag{17}$$

where $\dot{E_4}$ is the exergy exiting in the turbine, $\dot{E_5}$ is the exergy of the isobutane vapor entering the condenser, $\dot{E_8}$ is the exergy of saturated isobutane exiting the preheater, $\dot{E_7}$ is the exergy of isobutane entering the preheater, and $\dot{E_{PHX}}$ is the exergy destroyed in the preheater.

5.4 Condenser

Water-cooled condenser of the ORC cycle is used. The two-phase mixture entering the condenser is steam corresponding to the pressure at a temperature of 46.5 °C (DiPippo & Marcille, 1984; DiPippo, 2012). The exergy flow in the condenser is:

$$\dot{E_5} = \dot{E_6} + \dot{E_{11}} - \dot{E_{10}} + \dot{E_{CX}} \tag{18}$$

where $\dot{E_5}$ is the exergy of the isobutane vapor entering the condenser, $\dot{E_6}$ is the exergy of isobutane liquid exiting the condenser, $\dot{E_{10}}$ is exergy of cold water entering the condenser, $\dot{E_{11}}$ is the exergy of cooling water entering the cooling tower, and $\dot{E_{CX}}$ is the exergy destroyed in the condenser.

5.5 Working Fluid Pump

The work of a pump in any power plant is categorized as a parasitic or auxiliary load. Work has to be done in the system. The exergy of the working fluid pump shown is expressed as:

$$\dot{E}_6 = \dot{E}_7 + \dot{E}_{WPump} + \dot{E}_{PX} \quad (19)$$

where $\dot{E}_6$ is the exergy of isobutane liquid exiting the condenser, $\dot{E}_7$ is the exergy of compressed isobutane, $\dot{E}_{WPump}$ is the gross work of the pump, and $\dot{E}_{PX}$ is the exergy destroyed in the pump.

6. RESULTS AND DISCUSSION

The energy and exergy of the proposed binary power plant for Olkaria I were analyzed using EES code. The optimum conditions achieved for the maximum net work of the turbine were an evaporator pressure of 3123 kPa, condenser pressure of 627.3 kPa, and reinjection temperature of 85 °C. These conditions gave maximum net power of 2281 kW and a working fluid mass flow rate of 63.38 kg/s, with cycle, plant, and utilization efficiencies of 9.865%, 10.81%, and 31.70%, respectively (Table 4).

The optimized cycle parameters are presented in Table 5. The two pressures of the system are P_3 for Steps 3, 7, and 8 on the high-pressure side and P_4 for Steps 4, 5, and 6 on the low-pressure side. To arrive at the optimized value of P_3, low pressure was maintained at 627.3 kPa according to the condenser temperature T_5. Figure 5 shows the relationship between the turbine inlet pressure and the net work of the isobutane cycle. The optimum pressure is 3123 kPa, producing net turbine work of 2281 kW as illustrated in Figure 6.

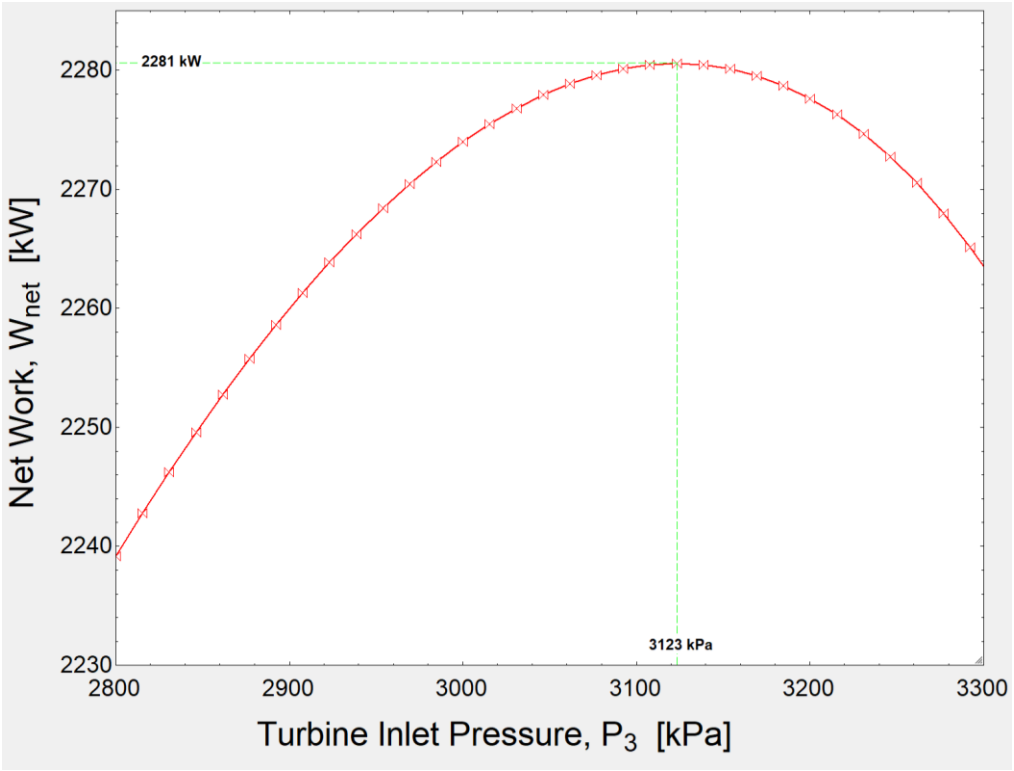

Figure 5: Relationship between the turbine pressure and net power.

Another critical parameter of the system is the reinjection temperature T_2, which is important in determining the working fluid flow rate in the ORC. With geothermal fluid in Olkaria having a low concentration of dissolved solids, the selected reinjection temperature requires a flow rate of 63.38 kg/s. The flow rate is calculated using EES code and a heat and mass balance in the evaporator with a pinch point of 5 K (DiPippo, 2012).

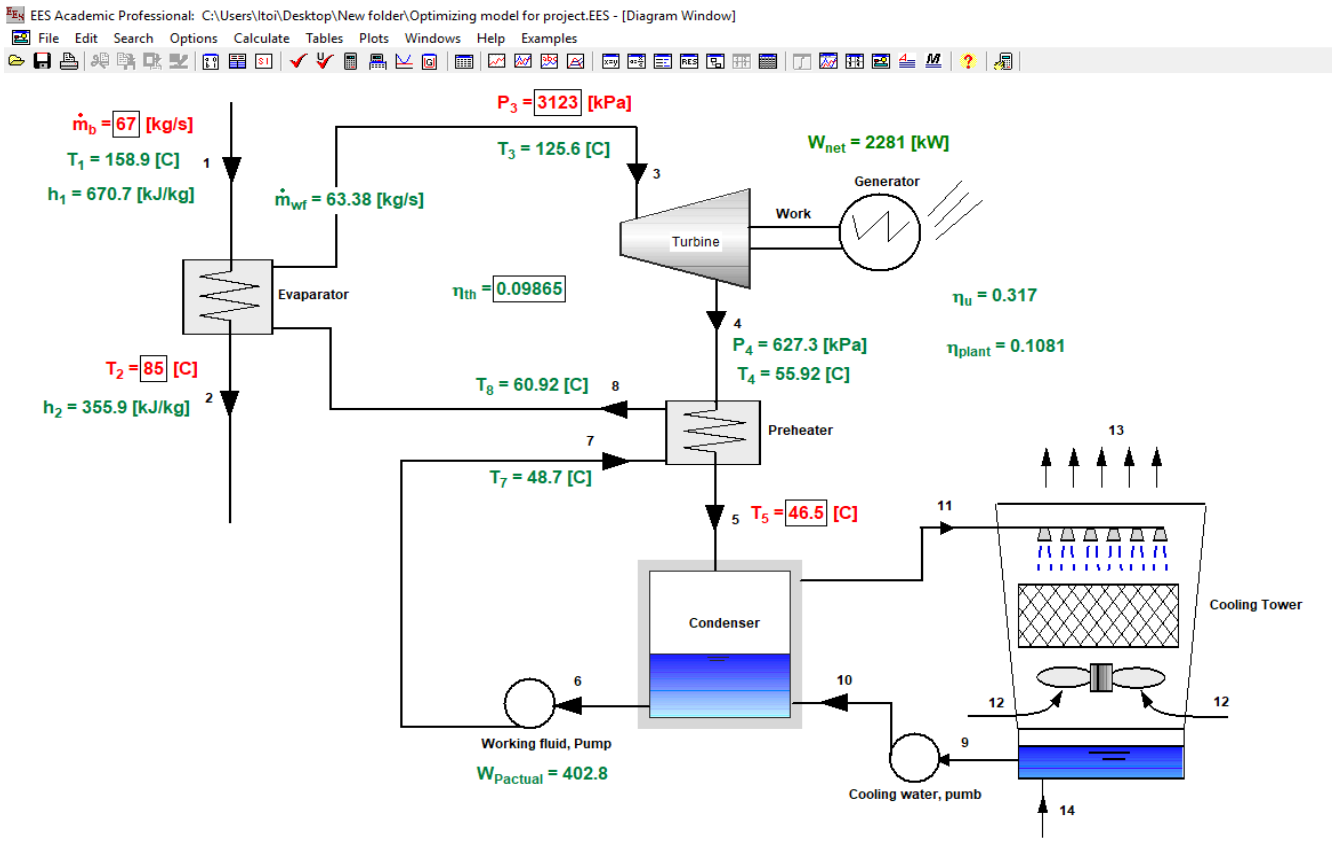

Figure 6: Optimization of the proposed ORC model using EES code.

Table 4: Summary of the optimized ORC cycle.

State	Fluid type	Phase	Pressure (kPa)	Temperature (^{0}C)	Enthalpy (kJ/kg)	Mass flow rate (kg/s)	Energy (kW)	Exergy(kW)
0	Brine	Dead State	86	25	83.93	-	-	-
0_b	Isobutane	Dead State	86	25	590.6	-	-	-
1	Brine	Liquid	600	158.9	670.6	67	44, 937	7,195
2	Brine	Liquid	57.81	85	355.9	67	23,846	1,763
3	Isobutane	Vapor	3123	125.8	684.7	63.38	43,407	8,703
4	Isobutane	Vapor	627.3	55.79	635.6	63.38	40,296	5,100
5	Isobutane	Vapor	627.3	46.5	616.9	63.38	39,098	4,985
6	Isobutane	Liquid	627.3	46.49	313.8	63.38	19,888	3,339
7	Isobutane	Liquid	3123	48.71	320.2	63.38	20,290	3,704
8	Isobutane	Liquid	3123	60.79	351.8	63.38	22,316	3,919

Considering the waste brine and the energy used by the evaporator, the second-utilization energy of the system was 41.98%.

Geothermal fluid from the separators with a mass flow rate of 67 kg/s at 158 °C had exergy of 7195 kW, with reference conditions of temperature of 25 °C and pressure of 86 kPa (Table 4)

Exergy destruction at different stages of the power plant is shown in the Grassman diagram of Figure 7. The exergy destroyed at each stage was calculated as a percentage of the total available geothermal exergy.

The brine reinjected at a temperature 85 °C had energy and exergy of 23,846 kW and 1763 kW, respectively, representing 53.065% and 24.5% of the total available energy and exergy in the geothermal fluid.

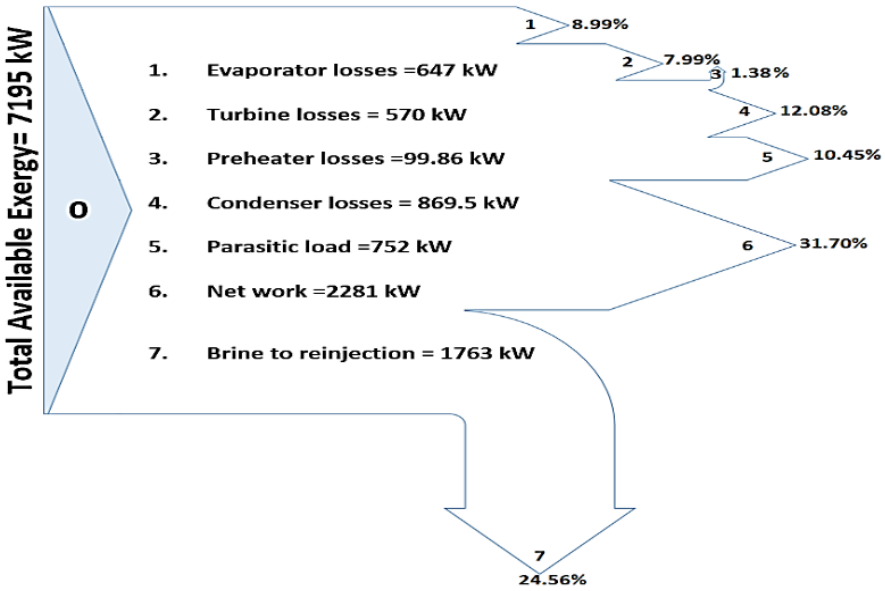

Figure 7: Grassman diagram of exergy flow of the binary plant.

7. CONCLUSION

Exergy and energy analysis of the proposed binary unit with isobutane as the working fluid showed the maximum power output was 2281 kW. The largest destruction of exergy was that in the condenser (12.08%) while the least was that in the preheater. The overall second-law efficiency of the project was 31.7% and the plant efficiency was 10.81%. The summary of the EES code simulation is illustrated in Table 5.

ACKNOWLEDGEMENTS

I acknowledge JICA, Kyushu University and JKUAT for giving me the opportunity to participate in the 2017 Geothermal Resource Engineers Course. I express my sincere gratitude to the lecturers, led by Prof. Fujimitsu and Prof. Itoi, for sharing their knowledge. Special thanks go to my supervisor Associate Prof. Saeid Jalilinasrabady for his guidance throughout the project. I am grateful to the 2017 geothermal group for the six months we had together. Last but not least, I thank my family for their encouragement and prayers. God bless you all.

NOMENCLATURE

C_b	specific heat capacity of water (kJ/kg K)
E_{input}	total exergy inflow to the control volume (kW)
$E_{desired}$	total desired exergy output (network output) (kW)
E_{waste}	sum of exergy from the system other than the desired exergy (kW)
$E_{destroyed}$	sum of exergy lost in the system as a result of irreversibility (kW)
EES	Engineers Equation Solver
$\dot{E}_{in}$	total available exergy entering the plant (kW)
GES	gas extraction system
GWP	global warming potential
h	enthalpy (kJ/kg)
$\dot{m}_b$	brine mass flow rate (kg/s)
$\dot{m}_{wf}$	working fluid mass flow rate (kg/s)
ODP	ozone depletion potential
P	pressure (kPa)
P_c	critical pressure (kPa)
P_s	saturation pressure (kPa)
Q	heat transfer rate (kW)
s	entropy (kJ/kg K)
T	temperature (°C)
T_c	critical temperature (°C)
W_{net}	net power output (kW)
W_p	work of the feed pump (kW)
W_t	power of the turbine (kW)
η_t	isentropic efficiency of the turbine (-)
η_{Plant}	overall plant efficiency (-)
η_p	efficiency of the pump (-)
$\dot{\theta}$	change in entropy (kJ/K)

REFERENCES

Anon., 2010. ***F- Chart Software, Engineering Equation Solver (EES).*** **[Online] Available at: http://www.fchart.com/ees/ [Accessed 2017].**

DiPippo, R., 2012. ***Geothermal Power Plants; Principles Applications, Case Studies and Enviromental Impact.*** **Third ed. s.l.:Elsevier.**

DiPippo, R., 2014. ***Geothermal power Plants, Principles, Applications, Case Studies and Enviromental Impact.*** **Fourth ed. s.l.:Elsevier.**

DiPippo, R. & Marcille, D. F., 1984. Exergy Analysis of Geothermal Power Plants. ***Geothermal Resource Council Transactions*****, August.**

Jalilinasrabady, S., 2011. Optimum Utilization of Geothermal Energy Employing Exergy Analysis and Resrvoir Simulation. ***Doctoral Dissertation*****.**

Jalilinasrabady, S., Itoi, R., Fujii, H. & Tanaka, T., 2010. ***Energy and Exergy Analysis of Sabalan Geothermal Power Plant.*** **Bali, s.n.**

Jalilinasrabady, S., Itoi, R., Hiroki, G. & Yamashiro, R., 2011. Exergetic Optimization of Proposed Takigami Binary Geothermal Power Plant, Oita, Japan. ***Geothermal Resource Council Transactions Vol 35*****, pp. 1305-1312.**

Jalilinasrabady, S. et al., 2012. Flash Cycle optimization of Sabalan geothermal power plant employing exergy concept. ***Geothermics,*** **Volume 43, pp. 75-82.**

Kumar, M. A., Naryan, D., Singh, R. & Vikas, G., 2016. Energy & Exergy Analysis of Thermal Power Plant. ***IJSRD-International Journal for scientific Research & Development,*** **4(03), pp. 2047-2052.**

Kwambai, B., 2010. ***Exergy Analysis of Olkaria I Power Plant, Kenya.*** **Bali, Indonesisa, s.n.**

Kwambai, B. C., 2005. ***Exergy analysis of Olkaria I Power Plant, Kenya,*** **Reykjavík, Iceland: United Nations University.**

Manente, G. & Lazzaretto, A., 2012. ***Compressibility factor as evaluation parameter of expansion processes in Organic Rankine Cycles.*** **Perugia, Efficiency, cost, optimization, simulation and environmental impact of energy systems (ECOS).**

Sadiq, J. Z. & Moon, H., 2014. Efficiency of Geothermal Power Plants: A worldwide view. ***Geothermics,*** **Volume 51, pp. 142-152.**

Yajing, Z. & Jianfeng, W., 2016. Exergoeconomic analysis and Optimization of a flash-binary geothermal power system. ***Applied Energy,*** **Volume 179, pp. 159-170.**

APPENDIX

Table 5: Results of 40 simulation runs with EES code to obtain the optimum turbine pressure, P_3.

EES Academic Professional: C:\Users\ltoi\Desktop\New folder\Optimizing model for project.EES - [Parametric Table]

File Edit Search Options Calculate Tables Plots Windows Help Examples

comprehehensive table | Table 2

1..40	1 p_4 [kPa]	2 $\dot{m}_{wf}$ [kg/s]	3 W_{net} [kW]	4 T_2 [C]	5 T_3 [C]	6 E_2 [kW]	7 η_{plant}	8 η_{th}	9 η_u	10 p_3 [kPa]
Run 1	627.3	63.61	2274	85	123.2	1763	0.1078	0.09755	0.316	3000
Run 2	627.3	63.6	2275	85	123.3	1763	0.1078	0.0976	0.3161	3005
Run 3	627.3	63.59	2275	85	123.4	1763	0.1079	0.09765	0.3162	3010
Run 4	627.3	63.58	2275	85	123.5	1763	0.1079	0.0977	0.3163	3015
Run 5	627.3	63.57	2276	85	123.6	1763	0.1079	0.09775	0.3163	3021
Run 6	627.3	63.56	2276	85	123.7	1763	0.1079	0.0978	0.3164	3026
Run 7	627.3	63.55	2277	85	123.8	1763	0.108	0.09785	0.3164	3031
Run 8	627.3	63.54	2277	85	123.9	1763	0.108	0.0979	0.3165	3036
Run 9	627.3	63.53	2278	85	124	1763	0.108	0.09795	0.3165	3041
Run 10	627.3	63.52	2278	85	124.1	1763	0.108	0.098	0.3166	3046
Run 11	627.3	63.51	2278	85	124.2	1763	0.108	0.09805	0.3166	3051
Run 12	627.3	63.5	2279	85	124.3	1763	0.108	0.09809	0.3167	3056
Run 13	627.3	63.49	2279	85	124.4	1763	0.108	0.09814	0.3167	3062
Run 14	627.3	63.48	2279	85	124.5	1763	0.1081	0.09819	0.3168	3067
Run 15	627.3	63.47	2279	85	124.6	1763	0.1081	0.09823	0.3168	3072
Run 16	627.3	63.46	2280	85	124.7	1763	0.1081	0.09828	0.3168	3077
Run 17	627.3	63.45	2280	85	124.8	1763	0.1081	0.09832	0.3169	3082
Run 18	627.3	63.44	2280	85	124.9	1763	0.1081	0.09836	0.3169	3087
Run 19	627.3	63.43	2280	85	125	1763	0.1081	0.09841	0.3169	3092
Run 20	627.3	63.42	2280	85	125.1	1763	0.1081	0.09845	0.3169	3097
Run 21	627.3	63.41	2280	85	125.2	1763	0.1081	0.09849	0.3169	3103
Run 22	627.3	63.41	2280	85	125.3	1763	0.1081	0.09853	0.3169	3108
Run 23	627.3	63.4	2281	85	125.4	1763	0.1081	0.09857	0.317	3113
Run 24	627.3	63.39	2281	85	125.5	1763	0.1081	0.09861	0.317	3118
Run 25	627.3	63.38	2281	85	125.6	1763	0.1081	0.09865	0.317	3123
Run 26	627.3	63.37	2281	85	125.7	1763	0.1081	0.09869	0.317	3128
Run 27	627.3	63.36	2281	85	125.8	1763	0.1081	0.09873	0.317	3133
Run 28	627.3	63.35	2280	85	125.9	1763	0.1081	0.09877	0.3169	3138
Run 29	627.3	63.34	2280	85	126	1763	0.1081	0.09881	0.3169	3144
Run 30	627.3	63.33	2280	85	126.1	1763	0.1081	0.09884	0.3169	3149
Run 31	627.3	63.32	2280	85	126.2	1763	0.1081	0.09888	0.3169	3154
Run 32	627.3	63.31	2280	85	126.3	1763	0.1081	0.09891	0.3169	3159
Run 33	627.3	63.3	2280	85	126.4	1763	0.1081	0.09895	0.3169	3164
Run 34	627.3	63.29	2280	85	126.5	1763	0.1081	0.09898	0.3168	3169
Run 35	627.3	63.28	2279	85	126.6	1763	0.1081	0.09902	0.3168	3174
Run 36	627.3	63.27	2279	85	126.7	1763	0.1081	0.09905	0.3167	3179
Run 37	627.3	63.26	2279	85	126.8	1763	0.108	0.09908	0.3167	3185
Run 38	627.3	63.25	2278	85	126.9	1763	0.108	0.09911	0.3167	3190
Run 39	627.3	63.24	2278	85	126.9	1763	0.108	0.09914	0.3166	3195
Run 40	627.3	63.23	2278	85	127	1763	0.108	0.09917	0.3166	3200

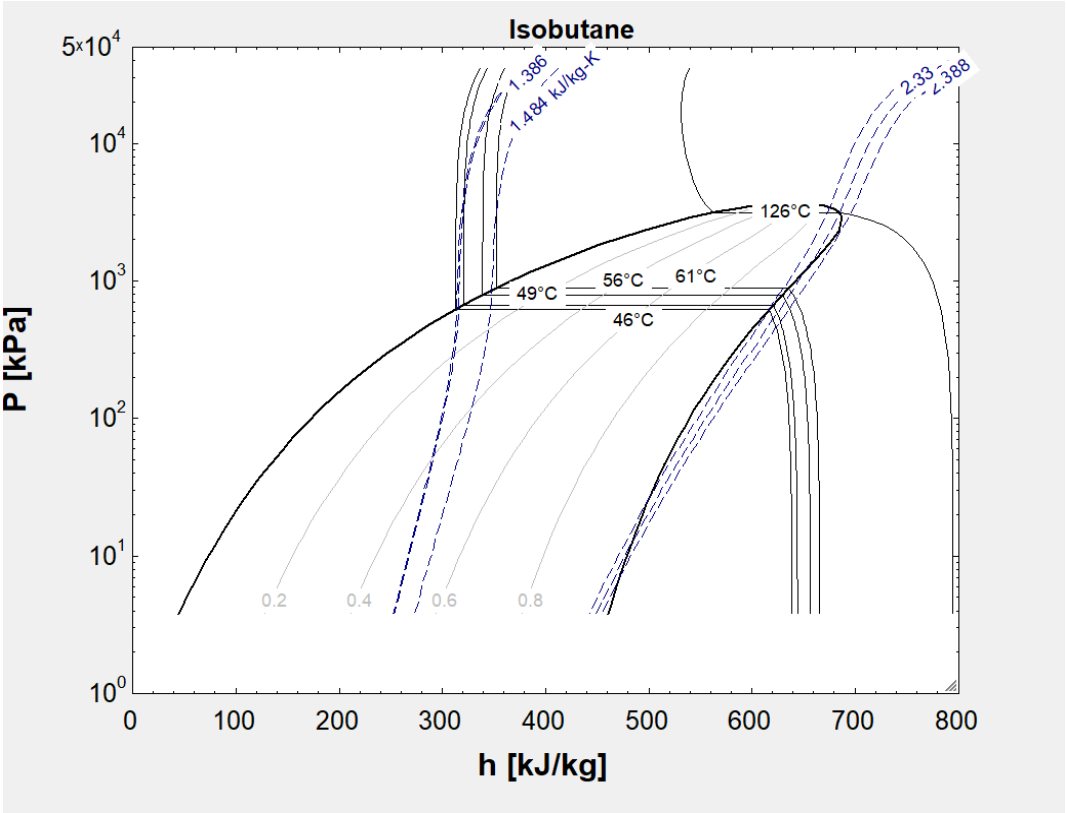

Figure 8: Pressure versus enthalpy of the optimized ORC cycle.